XRD studies of evolution of catalytic nickel nanoparticles during synthesis of filamentous carbon from methane

M.A. Ermakova *, D.Yu. Ermakov, L.M. Plyasova and G.G. Kuvshinov

Boreskov Institute of Catalysis, Prosp. Ak. Lavrentieva 5, Novosibirsk 630090, Russia
E-mail: erm@catalysis.nsk.su

Received 9 June 1999; accepted 2 September 1999

The XDR technique was used for studying a series of high-loaded (90%) nickel catalysts with silica as a textural promoter. These were catalysts for direct cracking of methane at 550 °C. A relation between the initial average size of active catalyst particles, carbon yield and average methane conversion was demonstrated. Genesis of these catalysts was studied including oxide precursors, reduced catalysts prior to the reaction, as well as catalysts upon their contacting the reaction medium for various periods of time from 15 min to 2 h. The active catalyst particles were shown to merge or disperse at the outset of the reaction depending on their initial size. Anyway, close average sizes ranging from 30 to 40 nm were observed by the end of the first reaction hour for all the catalytic systems providing the carbon yield of 300–385 g/g Ni. The catalytic system was shown to self-organize in the course of direct methane cracking, i.e., the catalyst particles transform in response to the reaction conditions. If the size of nickel particles cannot vary, these catalysts are inefficient for the given process.

Keywords: evolution of particles, nickel catalysts, methane cracking, filamentous carbon

1. Introduction

The process of hydrocarbon decomposition to produce carbon of a unique filamentous structure has attracted attention of many researchers. Metals of the iron group are used as catalysts for this process. Various kinds of carbon filaments and nanotubes have been observed among the carbonaceous reaction products [1–3]. Different modifications of the filamentous carbon, from fluff to pyrocarbon-like rigid mesoporous granules, can be obtained depending on the catalyst used and on the reaction conditions [4,5].

An interesting but poorly understood feature of this process is the evolution of catalytic particles during synthesis of carbon. Variations in their size and chemical composition result, eventually, in their deactivation. Seemingly, when the catalyst is introduced into the reaction medium, anomalous saturation with carbon happens to the catalytic particles to cause a number of phenomena. As a result, sometimes the metal particles merge with one another, and in the other cases disperse [6–9]. The behavior of the particles depends on the composition of the reaction medium and temperature [10]. The metal particles were discovered to reach a liquid-like state at unusually low temperatures (below 0.5 m.p.) under the action of carbon dissolved therein [11]. The reaction of hydrocarbon decomposition to produce catalytic filamentous carbon is sensitive to such factors as temperature, the catalyst composition, particle size of the dispersed phase, composition of the reaction medium, etc. One can say that the catalytic particle behaves like a living organism and, depending on the life conditions, can live for seconds to dozens of hours. The lifetime depends on a subtle equilibrium, violation of which results in the catalyst deactivation (death). Many researchers dealt with the driving force that makes the carbon migrating through the bulk of a catalytic particle from the sites of hydrocarbon adsorption and decomposition towards the sites of its aggregation in the form of graphite layers [12–16]. Anyway, the reasons for violation of this process are as yet not clearly understood. Either blocking the particles with a carbon coat impenetrable for reactants or particle disintegration in the course of the reaction may bear responsibility for the catalyst deactivation [6,8,9,17]. The particle size is among the most important factors affecting the lifetime of active catalytic particles. Conceivably, distinct reaction conditions need some optimal particle size to allow for the equilibrium between the rate of hydrocarbon decomposition and the rate of carbon filament growth to be maintained for the longest time.

The present work was aimed at studying, with the reaction of methane decomposition as an example, the evolution of nanoparticles of catalysts with different initial dispersion. Ni–SiO_2 was used as the model system. Nickel was chosen as the most active catalyst for methane decomposition, and silica as the textural promoter providing the minimal interaction with the active component. The nickel loading was 90% because high-loaded nickel catalysts are known to possess the longest lifetime in this reaction [18–20].

2. Experimental

A series of nickel oxide samples (table 1) were used for preparing catalysts. The preparation procedure was as fol-

* To whom correspondence should be addressed.

Table 1
Characteristics of samples of nickel oxide used for preparing nickel catalysts.

Sample of NiO	Specific surface NiO (m^2/g)	Pore volume of NiO ($s\,m^3/g$)	Average pore size of NiO, XRD data (nm)	Average size of NiO particles, XRD data (nm)
1	144	0.57	17	8
2	56	0.28	20	22
3	29	0.15	20	36
4	7	0.03	20	90
5	3	0.013	20	120

lows. Oxide samples were impregnated with a calculated quantity of an alcohol solution of tetraethoxysilane used as a silica supplier. The solution was subjected to partial prehydrolysis in an acid medium. More procedural details are given elsewhere [19,20]. Catalysts were dried at room temperature for 24 h and reduced in pure hydrogen at 550 °C for 2 h. To avoid pyrophoric phenomena, the catalysts to be unloaded from the reactor were passivated with ethanol and dried at room temperature. A series of 90% Ni–10% SiO_2 catalysts distinguished by the average size of active particles were thus prepared.

Textural characteristics of catalysts were studied by low-temperature nitrogen adsorption at 77 K using an automated ASAP-2400 installation.

X-ray powder diffraction patterns were recorded using a URD-63 diffractometer (Cu Kα radiation at $\lambda = 0.15418$ nm, a graphite crystal monochromator). Silicon was used as an internal reference. Coherent scattering regions for nickel oxide and nickel metal were determined by the Scherer equation [1] based on broadening of diffraction lines (200), (111) for NiO and (200), (111), (222) for Ni.

Catalysts were tested for methane decomposition at 550 °C using a laboratory fluidized bed installation equipped with a flow quartz reactor. The operative volume of the reactor was 20 cm^3. Methane was 99.99% purity, methane consumption was set at 120 liters per gram of nickel per hour for all runs. The outlet hydrogen concentration was determined by chromatography using a column filled with NaX zeolite. The catalyst activity was found from the hydrogen concentration in the reaction mixture. In order to study the behavior of the catalyst particles under the action of the reaction medium, the reactions were stopped in 15 min, 30 min, 1 h and 2 h for various samples. The sample weight was 0.04 g. Catalyst samples to be unloaded from the reactor were passivated.

The carbon yield (the amount of carbon deposited on the catalyst before it was deactivated) and the catalyst lifetime were determined by standing catalyst samples (0.01 g each in this case) under the reaction conditions as long as they were deactivated completely. The time taken for complete deactivation of reference samples was determined from the outlet hydrogen concentration, the reaction was stopped as soon as it reached 5%. Unloaded samples were weighed to determine the quantity of carbon deposited on the catalyst during the reaction.

The average methane conversion was calculated by the formula

$$X = \frac{22.4G/M(\mathrm{C})}{120t} \times 100\%,$$

where G is the yield (g/g Ni) of carbon deposited on a catalyst before deactivation, M(C) the carbon molar weight, t the reaction time (h) at a constant methane consumption equal to 120 l/h g Ni.

3. Results and discussion

Acidic hydrolysis of tetraethoxysilane in the presence of a substoichiometric amount of water produces, in the present case, its linear oligomers [22]. Impregnation of oxide samples with such a solution makes the particles enveloped into a mesh formed by these chains. The polysiloxane mesh subjected to further thermal treatment loses its organic constituent but keeps its structure while being transformed into silica, which behaves as a textural promoter. This method for catalyst preparation, unlike co-precipitation involving inevitable interaction between constituents, allows the probability of the chemical interaction to be minimized. The active component of co-precipitated catalysts can never be completely reduced due to an intimate interaction between the constituents at the precipitation stage. Thus, there are regions of local distortions in the metal crystal lattice induced by ions of the textural promoter. This state is also referred to as paracrystallinity [23–25]. Paracrystallinity was considered earlier in terms of potential improvement of the catalyst activity since, presumably, catalysis is more efficient when it proceeds over defect structures. As to the direct methane cracking, we suppose that this is exactly paracrystallinity, which causes the rapid deactivation to co-precipitated catalysts. The reason may be a decrease in the rate of carbon diffusion through regions of local distortions of a nickel crystal. For example, a co-precipitated nickel–alumina catalyst with 90% Ni loading and the average size of active particles corresponding to that of sample 1 provides ca. half carbon yield under similar reaction conditions [6]. The aim of our work is to reveal relations between the particles size and deactivation time of catalysts, hence, paracrystallinity as a factor affecting the deactivation should be excluded, if possible. For this purpose, we synthesized a model system in which an intimate interaction of the constituents can be hardly imagined.

Three trends in behavior of nanoparticles during reduction in the presence of silica can be seen from the data of table 2. For sample 1, there is observed ca. two times enlargement of generated Ni particles relative to the size of initial NiO particles. This effect can result from merging of the nickel metal particles during reduction. Therefore, this proportion of silica (10%) is evidently insufficient to provide stabilization of the fine NiO particles to be reduced to nickel. For sample 2, one can say about preserving the particle size in the course of the reduction. And, eventually,

Table 2
Correlation between average size of NiO, average size of Ni and carbon yield.

Catalyst sample	Average size, (200) line (nm)		Lifetime of catalysts (h)	Average methane conversion (%)	Carbon yield (g C/g Ni)
	NiO particles	Ni particles			
1	8	15	31	15	300
2	22	25	34	14.8	325
3	36	28	37	14.3	340
4	92	60	46	12.9	384
5	120	60	4	0.8	2

a progressing trend to dispersion of the particles is observed for samples 3–5 that may be attributed to the destruction of the large paternal oxide particle upon removal of oxygen followed by capturing the generated finer particles of nickel metal in the nodes of the SiO_2 lattice.

Sample testing for direct methane cracking revealed that samples 1–4 are close to one another in their capacity for accumulation of filamentous carbon. Nevertheless, as the averaged nickel metal particles increase in size, this capacity is seen to tend to some increase (from 300 to 384 g C/g Ni) at the corresponding decrease of the average methane conversion. Notice that approximately the same methane conversion equal to 16% is observed with samples 1–4 during the earliest stage of the reaction. Sample 5 differs from them by its short lifetime and an extremely low conversion. This fact seems strange if kept in mind that the coherent scattering region calculated for its particles from peak (200) is the same as that of sample 4.

The comparison of pre-reaction catalyst characteristics does not allow for the close carbon yields over samples 1–4 (even though the catalyst particles are considerably different in average size), as well as the sharp distinction between carbon yields obtained with samples 4 and 5 to be understood. One can try to explain these phenomena by tracing the catalyst transformations from the outset of the reaction. Therefore, we concentrated on the early hours of the catalyst lifetime when the carbon deposition did not hinder the XRD observations. The behavior of the 75% Ni–25% Al_2O_3 catalyst co-precipitated under similar conditions was studied earlier [6]. The initial average catalyst size, equal to 9 nm, was shown to increase to 40 nm through 3 h. Unfortunately, the study of this interesting phenomenon was limited to the only experiment. We believe that careful investigations of the behavior and evolution of catalytic particles throughout the reaction will elucidate the reasons for the catalyst deactivation in the course of such a complex process as synthesis of filamentous carbon by direct hydrocarbon cracking.

We followed the evolution of catalytic particles of a series of samples. The results obtained are summarized in figure 1 and table 3; they demonstrate that:

– the size of nickel particles of all the catalysts, except sample 5, undergoes noticeable changes as early as the first hour of the reaction;

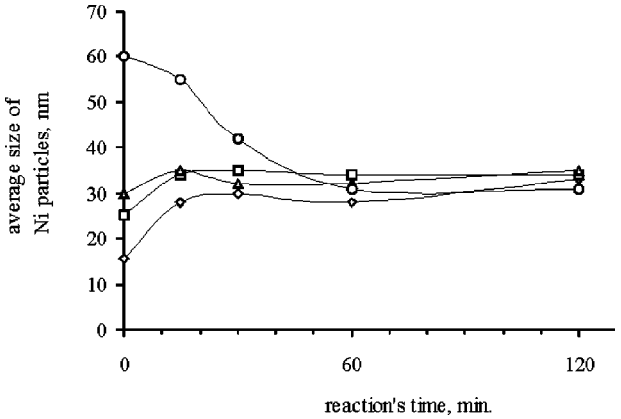

Figure 1. Evolution of nickel particles depending on the residence time in the reaction medium. (◊) Sample 1, (□) sample 2, (△) sample 3 and (○) sample 4.

Table 3
Variations in the average size of nickel particles (D_{Ni}) depending on the residence time in the reaction medium.

Catalyst sample	D_{Ni}					
	Initial	15 min	30 min	45 min	1 h	2 h
1	15–16	28	30	–	28	33
2	25	34	35	–	34	34
3	30	35	32	–	32	35
4	60	62	55	42	31	31
5	60	–	–	–	60	–

– the active evolution of nickel particles of samples 1–4 stops by the end of the first hour, practically no change is observed through the second hour;

– rather close particles size ranging between 30 and 35 nm is observed for all the samples except sample 5;

– a rapid (through 15 min) increase in average particles size is seen for samples 1–3;

– in contrast, dispersing of catalyst particles is observed for sample 4 throughout the first hour;

– no change is observed for particles of sample 5.

Thus, in the most cases the nickel catalysts may be considered as self-organizing systems in the reaction of methane decomposition. Nickel particles undergo active evolution to seek to some thermodynamically favorable size. There is visual merging of particles in samples 1–3. It is known that catalytic particles comprising iron group

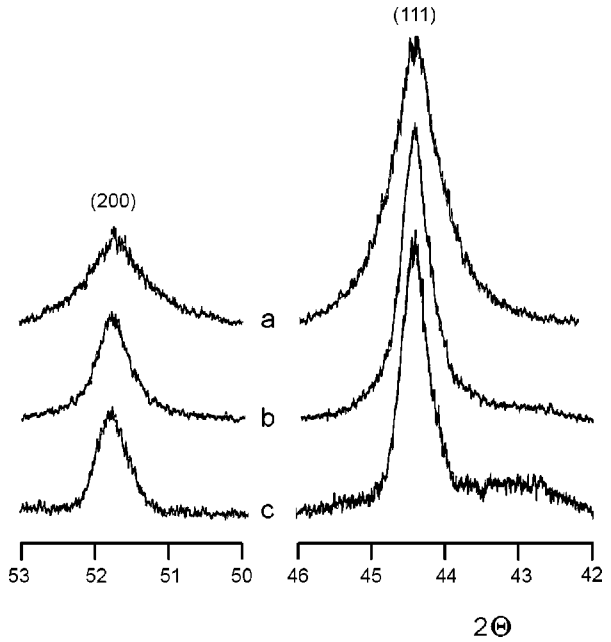

Figure 2. XRD patterns of sample 1 after exposure to methane cracking for: (a) 0, (b) 15 min and (c) 2 h.

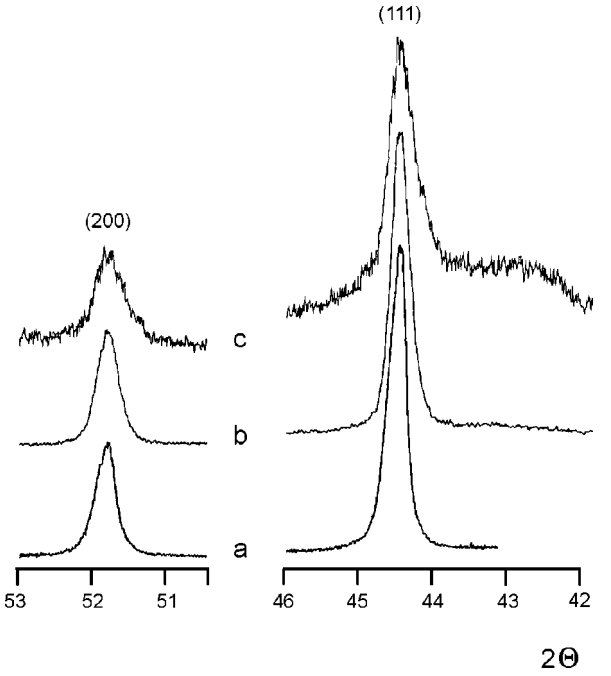

Figure 3. XRD patterns of sample 4 after exposure to methane cracking for: (a) 0, (b) 15 min and (c) 2 h.

metals are saturated with carbon upon their contacting an amorphous carbon and transformed into a liquid-like state at abnormally low temperature (600–700 °C) [11]. There is a currently debatable question on the lowest temperature for reaching such a state of the nickel particles during methane decomposition and on the manner in which this state relates to the particle size. The data we obtained indicate the liability of particles of initial size below 30 nm to merging. These particles have time to merge from the outset of the reaction before the filaments growing thereon separate them from one another. The XRD pattern recorded for sample 1 (figure 2) after its 15 min staying in the reaction medium shows evident narrowing of peaks (111) and (200). Hence, the average size of sample 1 particles changes towards larger values (15 to ca. 30 nm in the given case) as soon as the earliest minutes of the reaction.

The utter opposite of sample 1 is sample 4 which demonstrates the mechanism suggested by Sacco and coworkers [7] implying destruction of metal arrays consisting of fine crystals under the action of the dissolved carbon. The systems under discussion here are not the case of crystallite packages but, most likely, of individual crystals, which undergo dispersion when affected by chemical transformations to form carbide-like compounds. This process is longer and more uniform in time than merging; it takes about 1 h. The evolution of the average particle size is seen in the diffraction pattern of sample 4 (figure 3) from variations in the widths of peaks (111) and (200). It is unclear though why the dispersing stops when the average particle size reaches 30 nm, i.e., at the stop point of the merging particles of samples 1–3. Conceivably, the processes of merging and dispersing proceed concurrently in the catalyst throughout the total operation time. It is always probable that metal particles at the tips of growing filaments meet one another, hence the fine particles can merge whereas coarse particles, formed through merging, can disperse. Thus, the process turns about a certain average size determined by the reaction conditions. This is the case at ca. 30–40 nm average size.

The situation of sample 5 seems unclear. The coherent scattering regions, determined from peaks (111) and (200), are the same for samples 4 and 5, while they behave in different manners during the reaction. If turning to the data of table 2, one can see that the average size of the oxide precursor particles is much larger in sample 5 than in sample 4. Equal sizes of nickel particles (determined from peaks (111) and (200)) produced at the reduction does not mean similar behaviors of these samples. To elucidate the nature of this contradiction, diffraction patterns containing two order lines, viz. (111) and (222), were recorded for all of the catalyst samples. The line broadening is known to arise for a multiplicity of reasons (crystallite size, strain, and paracrystallinity), a different dependence of the integral width on the reflection order of plane arrays being observed. The broadening caused by the small size of the coherent scattering region is independent of the reflection order, whereas the presence of microstrains is proportional to it [23,25,26]. It was shown for sample 5 by comparing lines (111) and (222) in the diffraction pattern that defects are mainly responsible for broadening of line (111). Nickel of defect structure is likely to form in this case. A particle size (dispersion) equal to 140 nm was calculated for sample 5 according to the method proposed in [26]. Apparently, the catalyst with so much coarse particles is not effective for methane decomposition, since the violated equilibrium between the processes of formation of amorphous carbon and diffusion of this carbon to the sites of the graphite layer

aggregation results in rapid blocking of the overwhelming majority of catalyst particles by carbon growing thereon. The calculations for sample 4 showed no defect induced by microstrains; hence, broadening of line (111) in the diffraction pattern is caused by nothing but the dispersion. This is probably the reason for the highest carbon yield observed with this sample. As to samples 1–3, the line (111) broadening was mainly attributed to dispersion, although there are some defect.

4. Conclusions

Nickel catalysts consisting of active particles of various initial average sizes were shown to be effective for direct methane cracking to synthesize filamentous carbon. The potentiality of transformation of the active particles in response to the reaction conditions is the necessary condition. The major variations in the particle size occur at the earliest stage of the reaction (no longer than 60 min). The small-size particles were shown to tend to merging, whereas the large-size particles to dispersing. However, both processes result in formation of catalytic particles of the close size which is characteristic of the given reaction conditions, even though the initial particle sizes were different. We concluded based on the results obtained that the nickel catalysts introduced into methane at 550 °C behave as self-organizing systems. The optimal average size of the particles ranges between 30 and 40 nm under the given conditions.

Sintering of metal nanoparticless under the action of high temperatures and gas media is the subject of numerous studies. Different mechanisms of enlargement of initial particles are discussed, e.g., in [27,28]. At the same time, particle dispersing is a more rare phenomenon. It was mainly described for platinum, irridium supported on alumina [29,30]. The dispersion mechanism is not understood as yet. However, the reported behavior of catalytic particles cannot be referred to as the system self-organization because we treat the term *self-organization* as the occurrence of positive feedback, i.e., a catalytic system seek for a certain average particle size, which in its turns provides its longer lifetime. Probably, as was discussed earlier [11,31], the self-organizing behavior of catalytic systems is characteristic of the processes yielding the graphitized carbon among other products. The merging and dispersing of the active particles were assumed to proceed throughout the whole cycle of the catalyst operation. It seems probable that the catalyst deactivation happens as soon as the active particles are brought by the growing carbon filaments at so long distances that make it almost impossible for the particles to meet and merge. In this case the particle disintegration due to fragmentary dispersion or atomic erosion becomes irreversible. As a result, the internal balance in the particle is violated to cause poisoning it by the generated carbon. The size effect, among the other factors affecting the deactivation rate (reactant purity, the presence of local distortions of the crystal lattice of the metal catalyst, diffusion limitations imposed by the growth of carbon granules, etc.), is though to be the principal reason for deactivation.

Acknowledgement

The present work is supported by the Russian Foundation for Basic Research (Grant 98-03-32329).

References

[1] R.T.K. Baker, Carbon 27 (1989) 315.
[2] N.M. Rodriguez, J. Mater. Res. 8 (1993) 3233.
[3] N.M. Rodriguez, A. Chambers and R.T.K. Baker, Langmuir 11 (1995) 3862.
[4] G.G. Kuvshinov, Yu.I. Mogilnykh, D.G. Kuvshinov, D.Yu. Ermakov, M.A. Ermakova, A.N. Salanov and N.A. Rudina, in: *Symposium on Microscopic Studies of Coal and Carbon*, 22–27 August 1998, Prepr. Am. Chem. Soc. Div. Fuel Chem., Vol. 43 (1998) pp. 946–950.
[5] G.G. Kuvshinov, Yu.I. Mogilnykh, D.G. Kuvshinov, D.Yu. Ermakov, M.A. Ermakova, A.N. Salanov and N.A. Rudina, Carbon 37 (1999) 1239.
[6] L.B. Avdeeva, O.V. Goncharova, D.I. Kochubey, B.N. Novgorodov, L.M. Plyasova and Sh.K. Shaikhutdinov, Appl. Catal. A 141 (1996) 117.
[7] A. Sacco, Jr., P. Thacker, T.N. Chang and A.T.S. Chiang, J. Catal. 85 (1984) 224.
[8] E.G.M. Kuijpers, R.B. Tjepkema and J.W. Geus, J. Mol. Catal. 25 (1984) 241.
[9] C. Park and R.T.K. Baker, J. Catal. 179 (1998) 361.
[10] G.G. Kuvshinov, Yu.I. Mogilnikh, D.G. Kuvshinov, V.I. Zaikovskii and L.B. Avdeeva, Carbon 36 (1998) 87.
[11] O.P. Krivoruchko and V.I. Zaikovskii, Kinet. Katal. 39 (1998) 607.
[12] R.T.K. Baker, M.A. Barber, P.S. Harris, F.S. Feates and R.J. Waite, J. Catal. 26 (1972) 51.
[13] J.R. Rostrup-Nielsen and D.L. Trimm, J. Catal. 48 (1977) 155.
[14] R.A. Buyanov, V.V. Chesnokov, A.D. Afanasiev and V.S. Babenko, Kinet. Katal. 18 (1977) 1021.
[15] M.P. Manning, J.E. Garmirian and R.C. Reid, Ind. Eng. Chem. Process Des. Dev. 21 (1982) 404.
[16] J. Alstrup, J. Catal. 109 (1988) 241.
[17] J.B. Claridge, M.L.H. Green, S.C. Tsang, A.P.E. York, A.T. Ashcroft and P.D. Battle, Catal. Lett. 22 (1993) 299.
[18] O.V. Goncharova, L.B. Avdeeva, V.B. Fenelonov, L.M. Plyasova, V.V. Malakhov, G.S. Litvac and A.A. Vlasov, Kinet. Katal. 36 (1995) 293.
[19] M.A. Ermakova, D.Yu. Ermakov, G.G. Kuvshinov and L.M. Plyasova, Kinet. Katal. 5 (1998) 791.
[20] M.A. Ermakova, D.Yu. Ermakov, G.G. Kuvshinov and L.M. Plyasova, J. Catal., in press.
[21] A. Guinier, *Theorie et Technique de la Radiocristallographie* (Dunod, Paris, 1956).
[22] S. Sakka and K. Kamiya, J. Non Cryst. Solids 48 (1982) 31.
[23] C.J. Wright, C.G. Windsor and P.C. Puxley, J. Catal. 78 (1982) 257.
[24] W.S. Borghard and M. Boudart, J. Catal. 80 (1983) 194.
[25] A.M. Hindeleh and R. Hosemann, J. Phys. Chem. Solid State Phys. 21 (1988) 4155.
[26] L.M. Plyasova, Kinet. Katal. 33 (1992) 664.
[27] E. Ruckenstein and B. Pulvermacher, J. Catal. 29 (1973) 224.
[28] P. Wynblatt and N.A. Glostein, Prog. Solid State Chem. 9 (1974) 21.
[29] R.M.J. Fiedorow and S.E. Wanke, J. Catal. 43 (1976) 34.
[30] R.M.J. Fiedorow, B.S. Chahar and S.E. Wanke, J. Catal. 51 (1978) 193.
[31] V.N. Parmon, Catal. Lett. 42 (1996) 195.